AGU100 ADVANCING EARTH AND SPACE SCIENCE

Geophysical Research Letters

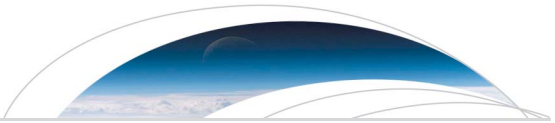

RESEARCH LETTER

10.1029/2018GL077950

Key Points:

- GNSS Wave Glider measures instantaneous sea surface heights with centimetric precision in the North Sea, in winds gusting up to 20 m/s
- Hourly dynamic ocean topography measurements agree with high-resolution assimilation model values to 6.1 cm standard deviation
- Measured significant wave heights agree with the WAVEWATCH III model and wave buoy data to 17–24 cm and dominant wave periods to 1.4 s

Correspondence to:
N. T. Penna,
nigel.penna@newcastle.ac.uk

Citation:
Penna, N. T., Morales Maqueda, M. A., Martin, I., Guo, J., & Foden, P. R. (2018). Sea surface height measurement using a GNSS Wave Glider. *Geophysical Research Letters*, *45*. https://doi.org/10.1029/2018GL077950

Received 24 FEB 2018
Accepted 23 MAY 2018
Accepted article online 29 MAY 2018

Sea Surface Height Measurement Using a GNSS Wave Glider

Nigel T. Penna[1], Miguel A. Morales Maqueda[2], Ian Martin[1], Jing Guo[1,3], and Peter R. Foden[4]

[1]School of Engineering, Newcastle University, Newcastle Upon Tyne, UK, [2]School of Natural and Environmental Sciences, Newcastle University, Newcastle Upon Tyne, UK, [3]Now at: GNSS Research Center, Wuhan University, Wuhan, China, [4]National Oceanography Centre, Liverpool, UK

Abstract To overcome spatial and temporal limitations of sea surface height instruments such as tide gauges, satellite altimetry, and Global Navigation Satellite Systems (GNSS) buoys, we investigate the use of an unmanned, self-propelled Wave Glider surface vehicle equipped with a geodetic GNSS receiver. Centimetric precision instantaneous sea surface height measurement is demonstrated from a 13-day deployment in the North Sea, during which the glider traversed a track of about 600 km. Ellipsoidal heights were estimated at 5 Hz using kinematic GNSS precise point positioning and, after correcting for tides using the Finite Element Solution 2014b model and for the geoid using the Earth Gravitational Model 2008, hourly dynamic ocean topography measurements agreed with those from the UK Met Office Forecasting Ocean Assimilation Model-Atlantic Margin Model 7 to 6.1-cm standard deviation. Conversely, on correcting for the tides and dynamic ocean topography, 5.1-cm standard deviation agreement with Earth Gravitational Model 2008 at its North Sea spatial resolution was obtained. Hourly measurements of significant wave height agreed with the WAVEWATCH III model and WaveNet buoy observations to 17 and 24 cm (standard deviation), respectively, and dominant wave periods to 1.4 s. These precisions were obtained in winds gusting up to 20 m/s.

Plain Language Summary High-rate (subsecond), continuous sea surface height measurement is demonstrated using an unmanned, self-propelled, surf-board sized Wave Glider surface vehicle equipped with a Global Navigation Satellite Systems (GNSS) receiver and antenna. GNSS data postprocessing determined centimetric precision sea surface heights over a user-defined, remotely piloted route of about 600 km in the North Sea over 13 days, measuring the waves and the variation in the sea surface from the geoid (the surface it would occupy due to Earth's gravity alone) caused by winds and currents, plus tides. Our portable, bespoke, in situ measurement method is applicable globally, subject to sufficient light for on-board instrumentation solar power, 10-m water depth, and GNSS signal tracking (outages attributed to waves breaking over the antenna arose when local winds became near gale force). The GNSS Wave Glider overcomes sea surface height measurement spatial resolution limitations of coastline-based tide gauges, single location GNSS buoys and ships following fixed routes, and the temporal and spatial resolution limitations of radar measurements from satellites. Such sea surface height measurements are needed for studies on coastal erosion; for the transport of sediments, pollutants, and heat; for understanding coastal ecosystems and climate change; and for coastal structural design and navigation management.

1. Introduction

Centimetric precision sea surface height (SSH) measurements are needed for determining (1) the dynamic ocean topography (DOT), (2) the marine geoid, (3) the sea state (waves), and (4) ocean tides. To date, SSH has been measured by altimetry satellites (e.g., Wunsch & Stammer, 1998), tide gauges, and geodetic Global Navigation Satellite Systems (GNSS) receivers on buoys (e.g., Xu et al., 2016), ships (e.g., Foster et al., 2009), and catamarans towed by small boats (Bonnefond et al., 2003). Altimetry satellites provide near global coverage but only at ~10 to 100-km spatial resolution and have coarse temporal resolution; for example, the Jason-1/2/3 repeat period is ~10 days. Furthermore, they can suffer from land contamination of the altimeter and radiometer signals in the coastal zone (e.g., Cipollini et al., 2017). Tide gauges provide high temporal resolution (up to ~1 s) but poor spatial resolution and are coastline-based. GNSS-based instruments can provide high temporal resolution (up to ~50 Hz), but buoys are pointwise measurements, while ships are usually constrained to commercial shipping lanes. Shipborne GNSS measurements must also account for variable

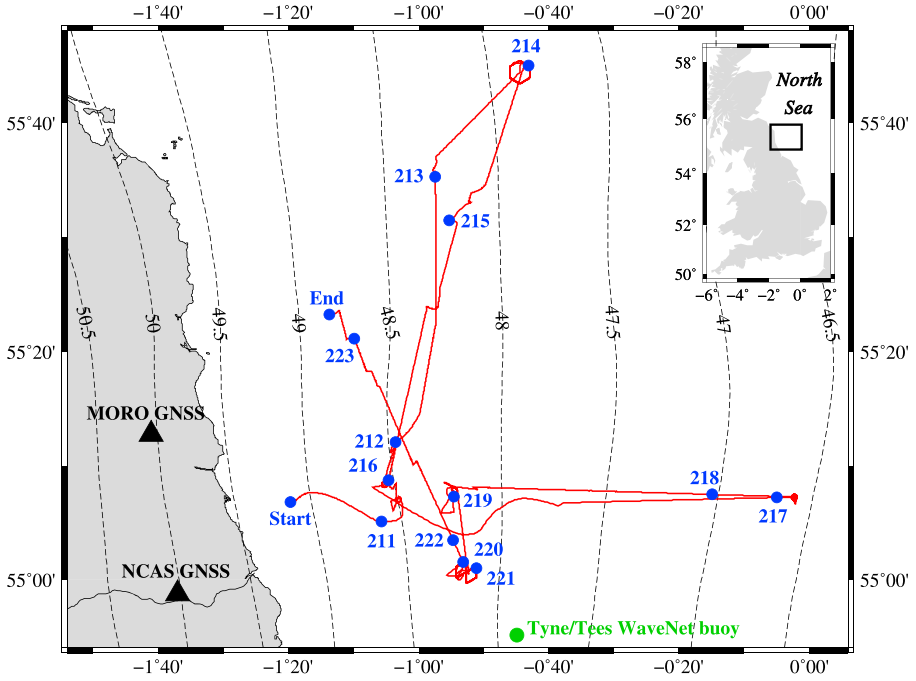

Figure 1. The Global Navigation Satellite Systems (GNSS) Wave Glider's track (red line) from launch at (55°08′N, 01°20′W) on 2016 day 210 to collection on day 223 (55°23′N, 01°14′W), with its location at 00:00 UTC on each day denoted by the blue circles and labels. The dashed lines represent EGM2008 geoid height contours in meters. Also shown are the locations of onshore GNSS reference stations and a WaveNet buoy. The inset box denotes the study region's location within Britain.

draft, squat effects (Roggenbuck et al., 2014) and cannot measure SSH directly, requiring radar measurements from the ship's deck to sea surface (e.g., Foster et al., 2014). Towed catamarans have route flexibility and overcome the variable draft limitation of ships but are restricted to short surveys because of fuel and crew limitations of the small towing boat, and local maritime regulations restrict the distance from shore that a particular category of small vessel may operate. Furthermore, such catamaran measurements are easily contaminated by the towing boat's wake. SSH has also been measured with airborne LiDAR in the coastal zone (Vrbancich et al., 2011), but such measurements are limited in spatial and temporal extent because of short flying times.

Unmanned marine surface vehicles equipped with geodetic GNSS receivers provide a means to overcome the deficiencies of the aforementioned sensors and platforms, enabling centimetric precision SSHs to be measured anywhere globally, at any temporal resolution. One such unmanned vehicle is the Liquid Robotics "Wave Glider SV2" (hereafter WG), comprising a float able to house a solar-powered instrumentation payload, connected by an umbilical cable to a subsurface wings/rudder frame, with the differential motion between the float and subsurface enabling wave-powered propulsion of up to ~1 m/s (~2 knots). The vehicle is only 2 m long so it can, in principle, measure waves as short as about 4 m wavelength and may be remotely piloted to go on any user-defined route (~10-m minimum depth requirement), with no restrictions on distance from the shore that it may travel or duration of survey as long as there is sufficient light for the solar panels. Added to our WG is a geodetic GNSS receiver and antenna, fixed on a mast above the float, thus maintaining a constant antenna to sea surface offset. This "GNSS WG" concept for precise water surface height determination was initially tested by Morales Maqueda et al. (2016). However, their short (24 hr) experiment was in the benign conditions of a lake, in the presence of light winds (3–5 m/s) and surface ripples/wavelets (amplitude 0.1–0.2 m). Furthermore, all on-board instrumentation above the GNSS antenna was removed, notably the meteorological mast, to ensure no GNSS antenna to satellite line-of-sight obstructions.

This paper investigates the use of the geodetic GNSS WG for SSH measurement with centimetric precision, via a 13-day experiment in the North Sea in a variety of sea states. It considers the detection and measurement precision of signals with both long wavelength (geoid and DOT) and short time scale (waves). Through

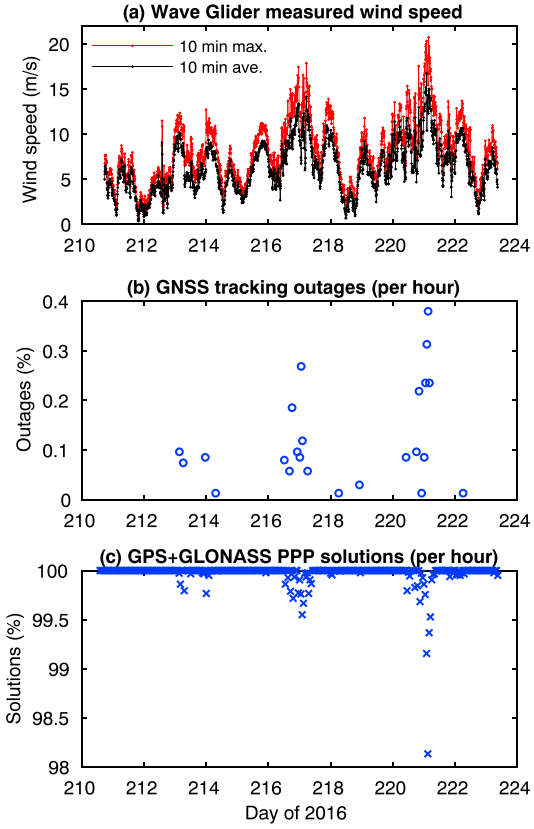

Figure 2. (a) Wave Glider-measured wind speed: maximum gust and average per 10 min. (b) Percentage of Global Navigation Satellite Systems 5-Hz epochs per hour for which signal tracking outages occurred. (c) Percentage of 5-Hz epochs per hour when a Global Positioning System + Globalnaya Navigatsionnaya Sputnikovaya Sistema precise point positioning solution with six or more satellites was obtained.

co-located wind speed measurements, it also investigates the meteorological conditions and sea states in which such signal measurement precisions are attainable. Finally, the potential applications of the GNSS WG instrument are discussed.

2. North Sea Experiment

A continuous deployment of a WG was undertaken from 28 July 2016 (day of year, hereafter denoted as "day," 210) to 10 August 2016 (day 223) in the North Sea. Deployment was from a small boat about 10 km off the coast of northeast England (55°07′N, 01°20′W), and the WG was remotely piloted via Iridium communications to various waypoints located as far as 81 km northeastward of the deployment location (55°44′N, 00°43′W) and 83 km eastward (55°07′N, 00°02′W), as shown in Figure 1. The entire WG track covered about 600 km and encompassed a wide range of geoid gradients, with the Earth Gravitational Model 2008 (EGM2008; Pavlis et al., 2012, 2013), suggesting a predominantly east-west gradient of ~3 cm/km (Figure 1). Wave heights ranged from submeter on day 210 to 3–4 m swell on days 222–223.

The WG payload included a Septentrio AsteRx-m GNSS receiver and PolaNt-x MF antenna, with L1 and L2 Global Positioning System (GPS) and Globalnaya Navigatsionnaya Sputnikovaya Sistema (GLONASS) code and carrier phase measurements collected continuously at 5 Hz from 13:22 UTC day 210 to 09:30 UTC day 223; an Airmar PB200 meteorological unit, collecting air pressure, temperature, and horizontal wind every 10 min, from a 1-m tall mast located at the center of the WG. To minimize GNSS signal obstructions from the meteorological mast, and automatic identification system and Iridium antennas, the GNSS antenna was installed astern, at a height of 0.35 m above the float. Winds at the time of deployment were light to moderate breeze (2–7 m/s) but increased to near gale force (gusting to 20 m/s) on day 221, before reducing to gentle to moderate breeze on days 222–223 (Figure 2). Also shown are GNSS signal tracking outages in hourly bins (commensurate with the hourly model results comparisons considered later), with epochs on which no GNSS measurements were recorded occurring in only 24 of 308 hourly bins over the 13 days. Tracking outages occurred a maximum amount of 0.38% (day 221), and it can be seen that most hourly bins with tracking outages coincided with times of ~15 m/s and above wind gusts, hence likely caused by locally generated wind waves breaking over the GNSS antenna. Two thirds of such hourly outages are below the 0.1% level and, on considering the 13-day data set as a whole, the percentage of 5 Hz epochs when GNSS data measurements were logged was 99.99%.

The 13 days of continuous 5 Hz GNSS data were postprocessed in precise point positioning (PPP) mode which, unlike relative GNSS positioning, is not dependent on data from a nearby reference station and can be applied anywhere worldwide. The Positioning And Navigation system Data Analyst (PANDA) scientific software (Liu & Ge, 2003) was used to generate a combined kinematic GPS + GLONASS float PPP solution, estimating per 5-Hz epoch the coordinates (using a process noise of 5,000 mm/√s) and GPS receiver clock offset (as a white noise parameter), hourly zenith wet delays (process noise of 20 mm/√s), time-constant ambiguities for both GPS and GLONASS, and a time-constant interfrequency bias per GLONASS satellite. Hence, observations from at least six satellites were needed every epoch to obtain a reliable position, with only such epochal position estimates used in the subsequent analysis. The ionosphere-free linear combination was used, with 2-cm observational standard deviation applied in the weighting of both the GPS and GLONASS phase observations and 2 m for both the GPS and GLONASS code observations. National Geodetic Survey phase center models were applied, and the Global Mapping Function (Boehm et al., 2006) used with a 7° elevation angle cut-off. Bespoke Wuhan University International GNSS Service Multi-GNSS Experiment Analysis

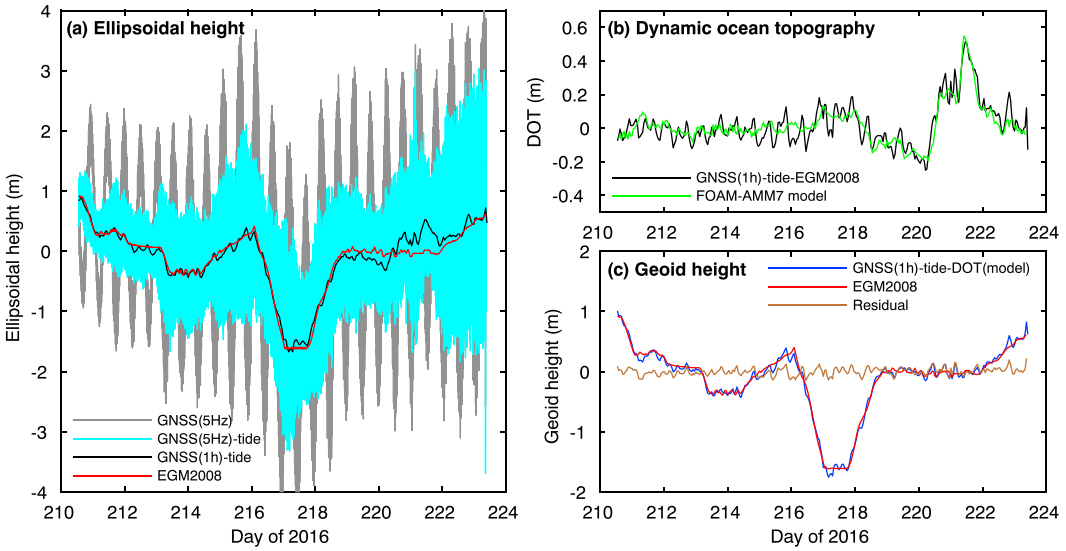

Figure 3. Global Navigation Satellite Systems (GNSS) Wave Glider-measured sea surface and geoid heights over time. (a) Ellipsoidal heights: Raw 5-Hz GNSS ellipsoidal heights and also tide-corrected (FES2014b model); hourly averaged tide-corrected GNSS heights; EGM2008 geoid heights. (b) Hourly dynamic ocean topography measured by GNSS above the EGM2008 geoid, and from the Forecasting Ocean Assimilation Model-Atlantic Margin Model 7 model. (c) Hourly GNSS-measured geoid heights and those from EGM2008 and their residual differences. All quantities are plotted about their respective medians.

Center satellite orbits and 30-s clocks (Guo et al., 2016) were generated using PANDA in 24 hr 50 min arcs and held fixed for the GPS + GLONASS data processed in 24-hr sessions, with the outputs concatenated to form an ellipsoidal height time series. The percentage of 5-Hz position solutions with six or more satellites available per hour and used are shown in Figure 2. The lowest solution availability of the 57 of the 308 hourly bins that did not have 100% solution availability was 98.1%, and coincided with the greatest proportion of tracking outages, with the availability for the other 56 hr all being greater than 99%. For the 13-day data set as a whole, 99.97% of the potential 5-Hz epochs were used for subsequent analysis.

To enable an assessment of the baseline height precision attainable from kinematic GNSS PPP processing in the region, 1-Hz data from the Ordnance Survey onshore static reference stations NCAS and MORO (Figure 1) were processed for days 210–223, using the same GPS + GLONASS approach as for the WG. Height standard deviations of 21 and 20 mm were obtained for NCAS and MORO, respectively, but as they are from static stations, should be considered optimistic precision indicators for the dynamic GNSS WG.

3. Dynamic Ocean Topography and Geoid Measurement

The 5-Hz GNSS-estimated ellipsoidal heights (median removed, as for all quantities here) are shown in Figure 3a. There is a prominent semidiurnal signal, commensurate with the M_2 tide amplitude of 1–2 m in the area (according to the Finite Element Solution 2014b model, FES2014b; Carrère et al., 2016), and longer time scale variability much larger than the 1.4 cm M_f and 0.8 cm M_m tidal amplitudes. Because the WG almost continuously moved along its track, and as the time series is too short to separate the main tidal constituents, we do not attempt to extract the tidal amplitudes and phase lags from the GNSS heights but correct for them using FES2014b and the hartid software (Agnew, 2012) to assess the GNSS WG's ability to detect geoid gradients, DOT, and waves. The tide-corrected GNSS ellipsoidal height time series is also shown in Figure 3a, with both high-frequency variability and longer time scale signals of up to 2–3 m apparent.

To interpret the longer time scale features of the tide-corrected GNSS ellipsoidal heights, 1-hr averages were computed, as shown in Figure 3a, together with EGM2008 geoid heights (used in the computation of recent geodetic mean DOT models, e.g., Mazloff et al., 2014) computed along the entire WG's track. While the DOT and geoid are difficult to separate, and extracting one requires modeling the other (e.g., Wunsch & Gaposchkin, 1980), the clear visual agreement with EGM2008 suggests that the dominant signal measured

is caused by spatial marine geoid variations as the WG moves along its track. For example, an ~2.0-m geoid change is detected on traveling ~67 km eastward from day 216 to 217 (Figure 1), and similarly ~1.7 m when the WG returns west along ~55 km of almost the same track from day 217 to 219 (~3-cm/km gradient). However, despite the WG traveling ~11 km parallel to the geoid contours from day 219 to 220, then remaining near-stationary from day 220 to 222, there are up to 0.5-m differences between the 1-hr averaged GNSS heights and the EGM2008 geoid from day 219 to 222.

To investigate the 1-hr averaged GNSS ellipsoidal SSH and EGM2008 geoid height discrepancies, particularly from day 219 to 222, the GNSS and geoid heights were differenced and compared with hourly ("instantaneous") DOT values computed from the UK Met Office Forecasting Ocean Assimilation Model-Atlantic Margin Model 7 (FOAM-AMM7). FOAM-AMM7 is based on the FOAM-Shelf model (O'Dea et al., 2012), which uses the Nucleus for a European Model of the Ocean (Madec, 2008) as its underlying ocean component and the NEMOVAR assimilation scheme (Waters et al., 2015). FOAM-AMM7 has a 7-km horizontal resolution and 1-hr temporal resolution from April 2014. The model is one-way nested to the Met Office global ocean model, includes 15 leading tidal constituents, and assimilates altimetry data in all domain areas where the ocean is deeper than 700 m.

The WG-measured (i.e., GNSS ellipsoidal SSH minus tide minus EGM2008 geoid height) and modeled DOT time series are shown in Figure 3b, with both showing a value of about −0.2 m around day 220, then an increase to about 0.5 m on day 221. This can be explained by an intensification of the northwesterly winds in the North Sea observed both in the FOAM-AMM7 model wind forcing and in the WG anemometer data, from about 3 m/s on day 219 to about 15 m/s on day 221 (Figure 2a). The strong winds led to water piling up in the central and southern North Sea. This analysis, together with both the measurements and model showing the same signals and the fact that the WG is near-stationary during days 220–221 (Figure 1) and hence the geoid height is near constant, strongly suggests that the GNSS and EGM2008 differences over days 220–221 shown in Figures 3a and 3b are caused by the DOT and not EGM2008 commission and omission errors. Smaller DOT values are obtained during the rest of the experiment. The standard deviation of the differences between hourly observed and modeled DOT is 6.1 cm.

To obtain WG-measured geoid heights, we subtracted the hourly modeled DOT from the tide-corrected hourly averaged GNSS ellipsoidal heights from the WG. The comparison with the EGM2008 geoid is shown in Figure 3c, with the residual largely constant, including for days 220–222. As EGM2008 is a static geoid to spherical harmonic degree 2190, which at latitude 55°N corresponds to a spatial resolution of ~5 km, to quantify the indicative spatial EGM2008 and WG-measured geoid height agreement, we thinned the measured geoid heights to ~5 km spacing along the WG track and synthesized EGM2008 geoid heights at these locations. The standard deviation of the differences is 5.1 cm, which is commensurate with the ~5-cm EGM2008 commission error estimates over the North Sea from Pavlis et al. (2008).

4. Wave Measurement

After correcting the raw 5-Hz GNSS ellipsoidal SSH measurements for the modeled tides, DOT and geoid, and removing the residual median, the remaining high-frequency signals represent the surface waves. The measured GNSS wave heights range from under 1 m on day 211 to about 4 m on day 223 (Figure 4a). The ability of the GNSS WG to measure the wave amplitude and period was quantified by computing hourly values of significant wave height (SWH; Figure 4b), defined as 4 times the standard deviation, and dominant wave period (Figure 4c), taken as the period with the greatest power in hourly Lomb-Scargle periodograms of the 5-Hz measured wave heights. These were then compared with modeled values (Saulter, 2017) computed hourly along the WG track using the daily predictions of the WAVEWATCH III 7-km Atlantic Margin Model (The WAVEWATCH III Development Group (WW3DG), 2016), as well as with 30-min values (averaged to 1 hr) from the Cefas Tyne/Tees WaveNet buoy, located south of the WG's track (Figure 1). The standard deviations of the hourly differences between the GNSS SWH values and those from the model and buoy over the 13 days were 17 and 24 cm, respectively (the respective RMS values were 18 and 24 cm), which included SWH ranging from ~0.5 m on days 210–212 to ~2.5 m on days 222–223. Meanwhile, the RMS and standard deviation of the dominant wave period differences were both 1.4 s with respect to both the model and buoy. Besides model errors and effects of the buoy not being coincident with the WG's track (notably on days 214, 217, and 223), these statistics will also include errors due to small amplitude signals caused by the

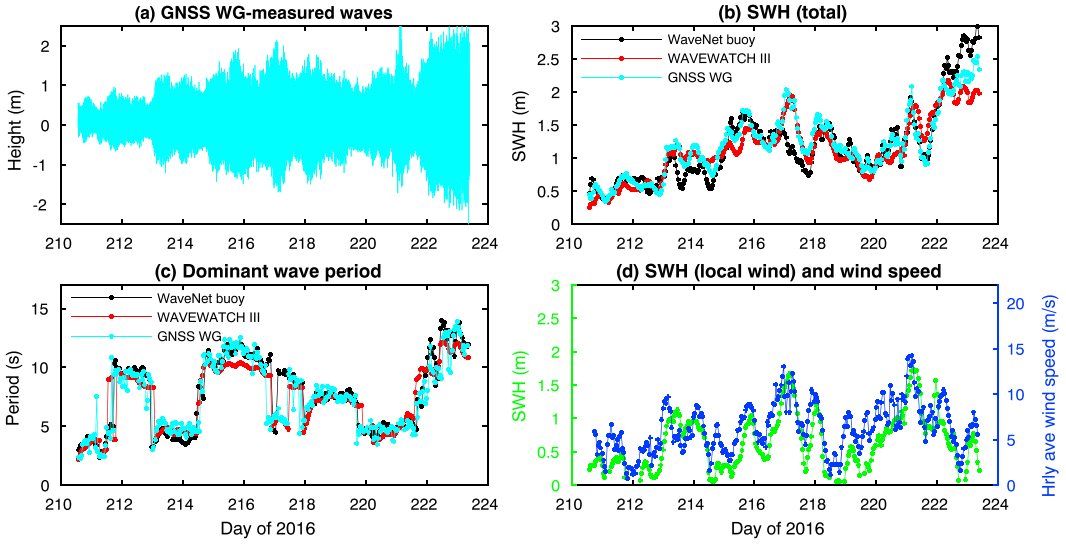

Figure 4. (a) Global Navigation Satellite Systems (GNSS) Wave Glider (WG)-measured waves (5 Hz); (b and c) hourly values of significant wave height (SWH) and dominant wave period respectively from the GNSS WG, WAVEWATCH III model (total), and WaveNet buoy; (d) hourly values of SWH from the WAVEWATCH III model (local wind wave component only) and hourly average WG-measured wind speeds.

unmodeled pitching and rolling of the WG's surface float as it responds to the wave field at the surface and to the dynamics of the subsurface glider. However, even for rather large inclination angles of 30°, the antenna elevation anomaly for an individual wave caused by these motions would amount to no more than 5 cm for the 0.35 m mast used here.

The largest SWHs occurred around day 222–223, with dominant wave periods of about 10–13 s, commensurate with swell periods, and swell is also suggested on days 215 and 216. Late on day 216 and during part of day 217, the dominant period drops abruptly from ~10 to ~5 s, suggesting locally generated wind waves. This corresponds to an increase in hourly average wind speed from ~5 m/s on day 216 to ~12 m/s on day 217, and similarly, there is a sharp increase in the WAVEWATCH III modeled SWH (wind wave component) from 0.5 to 1.5 m (Figure 4d). Similarly, during days 220–221, the dominant wave period is ~5 s, coinciding with local winds increasing from 7 to 15 m/s, but from the start of day 222, the winds gradually drop, and the dominant wave period gradually increases from 5-s wind waves to 10 to 13-s swell.

5. Conclusions and Outlook

We have demonstrated the ability of the unmanned GNSS WG to measure SSH in situ with centimetric precision using the kinematic GNSS PPP technique, which does not directly depend on land-based GNSS reference stations, so is applicable anywhere globally. Through a 13-day deployment in the North Sea, the GNSS WG's ability to measure the DOT and geoid to a precision of ~5–6 cm has been shown, and SWH and dominant wave period to 22–24 cm and 1.4 s, respectively, in winds gusting up to 20 m/s and with a maximum 10-min average of ~15 m/s. As an indication of how typical these wind conditions are of those elsewhere, the National Centers for Environmental Prediction Final Global Tropospheric Analysis product analysis of Arinaga and Cheung (2012) shows that 70–80% of the 10-m wind speeds across the oceans globally during 2000–2009 were less than ~15 m/s.

The new GNSS WG SSH instrument will be particularly useful in the coastal zone, bridging the gap between altimetry measurements which can suffer from land signal contamination, land-based tide gauges, and fixed-location GNSS buoys. It will enable satellite altimetry calibration at any point in the ocean, and the validation and improvement of ocean tide and DOT models, whose accuracy degrades over shelf seas and around complicated coastlines, as well as storm surge models and the marine geoid. For example, assuming the marine geoid is known, the deployment of the GNSS WG in a local area for several months, which is not practical with boats or ships, would enable the measurement of the mean DOT. Tides may be measured anywhere in the

ocean with the GNSS WG, including poleward of 66° (beyond the Jason-1/2/3 coverage), and it may enable the dynamics of amphidromic points to be measured, by continuously encircling them over long time scales. The SV2 WG measures surface currents (an AirMar CS4500 Ultrasonic water speed sensor is built-in), so combining these with the SSH measurements could potentially help separate the DOT from the geoid.

A fleet of GNSS WGs will enable the wave field to be measured in bespoke areas and the validation and improvement of wave field models. Besides its use in coastal erosion, sediment, and marine pollutant transport, the wave field is needed for climatology, as it controls the input of wind stress, heat, moisture, and atmospheric gases into the oceanic mixed layer. If a near real-time on-board GNSS processing capability were developed, transmitted SSH measurements could be used for sea state nowcasting for navigation, as well as the estimated tropospheric delays providing an additional source of offshore atmospheric water vapor for numerical weather prediction.

The GNSS WG is applicable to seafloor geodesy, as recognized by DeSanto et al. (2016), in the measurement and understanding of motions of the seabed, including tectonic motion, underwater volcanic uplift, coseismic motion, and motion around subduction zones. The position of a surface vehicle in a global reference frame is needed to determine the subsequent horizontal positions and motions of transponders on the sea bed via acoustic ranging (e.g., Chadwell & Spiess, 2008), or SSH measurements combined with bottom pressure measurements to determine height changes of the seafloor (e.g., Ballu et al., 2010). To date, the sea surface position has mainly been determined using GPS on ships, whose prohibitive costs limit their deployment above the particular sea floor location to short, infrequent durations, or buoys. The GNSS WG can be frequently deployed and can keep station to enable continuous measurement, acting as a buoy. With an echo sounder, the GNSS WG will be useful for bathymetric mapping to help determine ocean currents and mixing, as well as for monitoring sediment dynamics.

Acknowledgments
Thanks to Liam Rogerson, Neil Armstrong, Barry Pearson, Jeff Pugh, Paolo Cipollini, Colin Bell, and Jeff Polton for fieldwork or planning help; Duncan Agnew for hartid; Wuhan University for PANDA; and Will Featherstone, Phil Woodworth, and Xingxing Li for helpful discussions. The work was funded by NERC grants NE/K005421/1 and NE/K005944/1. We thank Ray Mahdon and Andrew Matthew for FOAM-AMM7 data and advice, respectively; CNES for FES2014b; Copernicus Marine Environment Monitoring Service for wind and model data; Cefas for WaveNet buoy data; and NERC BIGF for GNSS reference station data. See doi: 10.5281/zenodo.1250342 for the WG GNSS and wind speed data.

References

Agnew, D. C. (2012). SPOTL: Some programs for ocean-tide loading. SIO Technical Report, Scripps Institution of Oceanography.

Arinaga, R. A., & Cheung, K. F. (2012). Atlas of global wave energy from 10 years of reanalysis and hindcast data. *Renewable Energy*, *39*(1), 49–64. https://doi.org/10.1016/j.renene.2011.06.039

Ballu, V., Bouin, M.-N., Calmant, S., Folcher, E., Bore, J.-M., Ammann, J., et al. (2010). Absolute seafloor vertical positioning using combined pressure gauge and kinematic GPS data. *Journal of Geodesy*, *84*(1), 65–77. https://doi.org/10.1007/s00190-009-0345-y

Boehm, J., Niell, A., Tregoning, P., & Schuh, H. (2006). Global Mapping Function (GMF): A new empirical mapping function based on numerical weather model data. *Geophysical Research Letters*, *33*, L07304. https://doi.org/10.1029/2005GL025546

Bonnefond, P., Exertier, P., Laurain, O., Menard, Y., Orsoni, A., Jeansou, E., et al. (2003). Leveling the sea surface using a GPS-catamaran. *Marine Geodesy*, *26*(3), 319–334. https://doi.org/10.1080/714044524

Carrère, L., Lyard, F., Cancet, M., Guillot, A., & Picot, N. (2016). FES 2014, a new tidal model—Validation results and perspectives for improvements. ESA Living Planet Conference, Prague.

Chadwell, C. D., & Spiess, F. N. (2008). Plate motion at the ridge-transform boundary of the south cleft segment of the Juan de Fuca Rridge from GPS—Acoustic data. *Journal of Geophysical Research*, *113*, B04415. https://doi.org/10.1029/2007JB004936

Cipollini, P., Calafat, F. M., Jevrejeva, S., Melet, A., & Prandi, P. (2017). Monitoring sea level in the coastal zone with satellite altimetry and tide gauges. *Surveys in Geophysics*, *38*(1), 33–57. https://doi.org/10.1007/s10712-016-9392-0

DeSanto, J. B., Sandwell, D. T., & Chadwell, C. D. (2016). Seafloor geodesy from repeated sidescan sonar surveys. *Journal of Geophysical Research: Solid Earth*, *121*, 4800–4813. https://doi.org/10.1002/2016JB013025

Foster, J., Li, N., & Cheung, K. F. (2014). Sea state determination from ship-based geodetic GPS. *Journal of Atmospheric and Oceanic Technology*, *31*(11), 2556–2564. https://doi.org/10.1175/JTECH-D-13-00211.1

Foster, J. H., Carter, G. S., & Merrifield, M. A. (2009). Ship-based measurements of sea surface topography. *Geophysical Research Letters*, *36*, L11605. https://doi.org/10.1029/2009GL038324

Guo, J., Xu, X., Zhao, Q., & Liu, J. (2016). Precise orbit determination for quad-constellation satellites at Wuhan University: Strategy, result validation, and comparison. *Journal of Geodesy*, *90*(2), 143–159. https://doi.org/10.1007/s00190-015-0862-9

Liu, J., & Ge, M. (2003). PANDA software and its preliminary result of positioning and orbit determination. *Wuhan University Journal of Natural Sciences*, *8*, 603–609.

Madec, G. (2008). NEMO ocean engine: Note Du Pôle de Modél, Institut Pierre-Simon de Laplace (IPSL), France, No 27.

Mazloff, M. R., Gille, S. T., & Cornuelle, B. (2014). Improving the geoid: Combining altimetry and mean dynamic topography in the California coastal ocean. *Geophysical Research Letters*, *41*, 8944–8952. https://doi.org/10.1002/2014GL062402

Morales Maqueda, M. A., Penna, N. T., Williams, S. D. P., Foden, P. R., Martin, I., & Pugh, J. (2016). Water surface height determination with a GPS Wave Glider: A demonstration in Loch Ness, Scotland. *Journal of Atmospheric and Oceanic Technology*, *33*(6), 1159–1168. https://doi.org/10.1175/JTECH-D-15-0162.1

O'Dea, E. J., Arnold, A. K., Edwards, K. P., Furner, R., Hyder, P., Martin, M. J., et al. (2012). An operational ocean forecast system incorporating NEMO and SST data assimilation for the tidally driven European north-west shelf. *Journal of Operational Oceanography*, *5*(1), 3–17. https://doi.org/10.1080/1755876X.2012.11020128

Pavlis, N. K., Holmes, S. A., Kenyon, S. C., & Factor, J. K. (2012). The development and evaluation of the Earth Gravitational Model 2008 (EGM2008). *Journal of Geophysical Research*, *117*, B04406. https://doi.org/10.1029/2011JB008916

Pavlis, N. K., Holmes, S. A., Kenyon, S. C., & Factor, J. K. (2008). An earth gravitational model to degree 2160: EGM2008. European Geosciences Union General Assembly 2008, Vienna, Austria.

Pavlis, N. K., Holmes, S. A., Kenyon, S. C., & Factor, J. K. (2013). Correction to "The development and evaluation of the Earth Gravitational Model 2008 (EGM2008)". *Journal of Geophysical Research: Solid Earth*, *118*, 2633. https://doi.org/10.1002/jgrb.50167

Roggenbuck, O., Reinking, J., & Harting, A. (2014). Oceanwide precise determination of sea surface height from in-situ measurements on cargo ships. *Marine Geodesy*, *37*(1), 77–96. https://doi.org/10.1080/01490419.2013.868385

Saulter, A. (2017). North West European Shelf Production Centre, NORTHWESTSHELF ANALYSIS FORECAST WAV 004 012. CMEMS-NWS-QUID-004-012, pp. 28.

The WAVEWATCH III Development Group (WW3DG) (2016). User manual and system documentation of WAVEWATCH IIIR version 5.16 (Tech. Note 329, pp 326+ Appendices). NOAA/NWS/NCEP/MMAB, College Park, MD.

Vrbancich, J., Lieff, W., & Hacker, J. (2011). Demonstration of two portable scanning LiDAR systems flown at low-altitude for investigating coastal sea surface topography. *Remote Sensing*, *3*(9), 1983–2001. https://doi.org/10.3390/rs3091983

Waters, J., Lea, D. J., Martin, M. J., Mirouze, I., Weaver, A., & While, J. (2015). Implementing a variational data assimilation system in an operational 1/4 degree global ocean model. *Quarterly Journal of the Royal Meteorological Society*, *141*(687), 333–349. https://doi.org/10.1002/qj.2388

Wunsch, C., & Gaposchkin, E. M. (1980). On using satellite altimetry to determine the general-circulation of the oceans with application to geoid improvement. *Reviews of Geophysics*, *18*, 725–745. https://doi.org/10.1029/RG018i004p00725

Wunsch, C., & Stammer, D. (1998). Satellite altimetry, the marine geoid, and the oceanic general circulation. *Annual Review of Earth and Planetary Sciences*, *26*(1), 219–253. https://doi.org/10.1146/annurev.earth.26.1.219

Xu, X.-Y., Xu, K., Shen, H., Liu, Y.-L., & Liu, H.-G. (2016). Sea surface height and significant wave height calibration methodology by a GNSS buoy campaign for HY-2A altimeter. *IEEE Journal of Selected Topics in Applied Earth Observations and Remote Sensing*, *9*(11), 5252–5261. https://doi.org/10.1109/JSTARS.2016.2584626